Polym. Bull. (2011) 66:991–1004
DOI 10.1007/s00289-010-0408-5

ORIGINAL PAPER

Polycarbonate reinforced with silica nanoparticles

A. S. Luyt · M. Messori · P. Fabbri · J. P. Mofokeng · R. Taurino · T. Zanasi · F. Pilati

Received: 9 December 2009 / Revised: 7 June 2010 / Accepted: 7 November 2010 /
Published online: 23 December 2010

Abstract Nanocomposites of polycarbonate (PC) reinforced with nanosized silica particles were prepared by a melt mixing technique in an internal mixer. Two kinds of commercial hydrophilic fumed silicas differing in their specific surface area were added in amounts up to 5% by volume, and their reinforcing action was compared to that of organically modified silica, loaded in the same amounts. Particle–matrix interactions were investigated by means of rheological and dynamic-mechanical thermal analysis, demonstrating the important role played by the organic modification in the interactions with the polymer matrix, and showing an optimal nanoparticle loading around 2 vol%. The scratch resistance of the nanocomposites obtained from hydrophilic silicas was investigated, and a remarkable enhancement in the indenter's penetration resistance was observed for all the compositions with respect to pristine PC. The same behaviour was observed for the Shore D hardness and for the impact resistance of the nanocomposites that also significantly improved with the maximum load shifting from a minimum value of 521 N for pristine PC up to values grater than 1330 N for the nanocomposites, demonstrating the activation of effective mechanisms of energy dissipation due to the presence of the nanofillers.

A. S. Luyt (✉) · J. P. Mofokeng
Department of Chemistry, University of the Free State (Qwaqwa Campus),
Private Bag X13, Phuthaditjhaba 9866, South Africa
e-mail: LuytAS@qwa.ufs.ac.za

M. Messori · P. Fabbri · R. Taurino · T. Zanasi · F. Pilati
Dipartimento di Ingegneria dei Materiali e dell'Ambiente, Università di Modena e Reggio Emilia,
Via Vignolese 905/a, 41125 Modena, Italy

M. Messori · P. Fabbri · R. Taurino · T. Zanasi · F. Pilati
Consorzio Interuniversitario Nazionale di Scienza e Tecnologia dei Materiali,
INSTM, Via Giusti 9, 50121 Florence, Italy

Keywords Polycarbonate · Silica nanoparticles · Impact and scratch resistance · Dynamic mechanical properties

Introduction

Polycarbonate (PC) is amongst the most important thermoplastics for a wide variety of applications, especially in cases where optical clarity is important and conspicuous mechanical properties are required. Several approaches have been presented for the modification of this polymer, aimed at extending and widening its application within the engineering field without affecting its transparency. In recent years, the vast majority of the scientific efforts have been dedicated to the preparation and characterization of the relative nanocomposites obtained by inclusion of nano-objects of different nature, due to the fact that the addition of well-dispersed nanofillers to transparent polymer matrices could preserve their optical clarity with the additional improvement of stiffness, impact resistance and scratch resistance. All these have been compelling reasons for investigating PC-based nanocomposites. Several manufacturing approaches have been described for their preparation that can be classified into three main categories: in situ polymerization of the monomers in the presence of the inorganic nanoparticles, in situ particles generation in the presence of the polymer or polymer precursors, and melt compounding.

In the context of industrial applications, the third method certainly represents the preferred and most convenient method for nanocomposites preparation; it has been successfully applied to the preparation of PC clay nanocomposites [1–5]; thermally and electrically conductive PC [6–9] composites containing carbon nanotubes; functional nanocomposites with metal-based nanoparticles (Al_2O_3, ZnO, ZnS, PbS) [10, 11] or with polyhedral oligomeric silsesquioxane POSS [12].

Amongst the wide set of nano-fillers used for PC modification, particular interest has been drawn by nano-silicas (SiO_2), thanks to the commercial availability of several fumed products characterized by different surface area and porosity, or the ease of production of spherical nanoparticles through sol–gel techniques or hydrothermal reactions. Nanoscopic SiO_2 has been used particularly for the improvement of thermal and chemical stabilities of PC [13] and PMMA, and the effect of organic surface functionalization to avoid aggregation when particles are integrated in the hydrophobic matrix has been widely discussed and reviewed, also in a recent paper [14].

There is only limited information in the literature concerning the possibility to further enhance the mechanical properties of transparent polymer matrices such as PC or PMMA by direct incorporation of unmodified hydrophilic nano-SiO_2 through melt compounding, even though this approach could be particularly convenient for very demanding applications where optical transparency and outstanding impact properties and scratch resistance are required. Therefore, the main objective of this study is to explore the effect of small amounts of nanosized SiO_2 particles on the impact properties, scratch resistance and dynamic mechanical properties of a transparent PC matrix; this article demonstrates that impressive enhancements can

be obtained even by direct compounding of SiO_2 nanofillers within the polymer melt by melt mixing, without the need of organic surface functionalization of the inorganic nanoparticles.

Experimental details

Materials

Commercial grade bisphenol-A polycarbonate (PC, Makrolon® 2407 produced by Bayer MaterialScience, Germany, and having a melt flow rate at 300 °C/1.2 kg of 20 g/10 min) was used in pellet form. Before processing the resin was dried at 120 °C overnight under static vacuum.

AEROSIL® 90 (A90, produced by Degussa, Germany) is a hydrophilic fumed silica with a specific surface area of 90 $m^2\ g^{-1}$ and an average primary particle size of 20 nm. AEROSIL® 380 (A380, produced by Degussa, Germany) is a hydrophilic fumed silica with a specific surface area of 380 $m^2\ g^{-1}$ and an average primary particle size of 7 nm. Both silicas were used as received, after drying at 120 °C under static vacuum for a minimum of 16 h, without any further surface modification. These nanoparticles were selected to explore the effect of very different surface areas and average primary particle sizes on the reinforcement effect in PC.

AEROSIL® R972 (R972, produced by Degussa, Germany) is a hydrophobic silica having chemically surface-bonded methyl groups, based on a hydrophilic fumed silica with a specific surface area of 130 $m^2\ g^{-1}$ and an average primary particle size of 16 nm. These nanoparticles were selected to explore the effect of surface organophilic modification on the interactions with the polymer matrix. This silica was also dried at 120 °C under static vacuum for a minimum of 16 h before further use.

Melt processing

Composites were prepared by melt mixing using a PolyLab Rheomix R600 internal mixer (Thermo Haake) equipped with roller rotors. The standard blending procedure was as follows: Pelletized PC (about 40 g) was charged in the internal mixer chamber and softened at a temperature of 240 °C. SiO_2 nanoparticles (concentration in the range from 0 to 5% by volume) were added after torque stabilization (typically 10 min after feeding). The rotors speed was set at 60 rpm and the mixing time was kept equal to 30 min for all samples.

In order to verify the thermal stability of the organic surface modification of R972 silica, differential thermal analysis and thermogravimetric analysis were carried out on R972 both under oxygen or nitrogen atmospheres. No weight loss or endothermic or exothermic peaks attributable to decomposition of the organic components were observed in the temperature range from room temperature to 300 °C, confirming the required stability of R972 in the used processing conditions.

After melt mixing, sheets having dimensions of $50 \times 50 \times 4$ mm^3 were compression moulded using a hot-plate press (Carver Inc., IN, USA) operating at a temperature of 240 °C, and punch-cut specimens were obtained.

PC without SiO_2 nanoparticles was processed under the same experimental conditions for comparison.

In the following discussion the prepared samples will be identified with the code pristine polycarbonate (PC), or PC_type of silica nanoparticles_vol% (example: PC_A90_1 refers to the nanocomposite containing 1 vol% of AEROSIL® 90 nanoparticles).

Nanocomposites characterization

The glass transition temperature (T_g), elastic modulus (E'), loss modulus (E'') and loss factor (tanδ) were determined through dynamic mechanical thermal analysis (DMTA) using a Diamond DMA (Perkin Elmer); specimens ($52 \times 12 \times 1$ mm^3) were tested in bending mode at a constant frequency of 1 Hz, while heated from 40 to 200 °C at a rate of 5 °C min^{-1} under nitrogen gas.

Differential scanning calorimetry (DSC) was carried out in a DSC2010 (TA Instruments) to determine T_g values in comparison with DMTA, using a heating scan rate of 10 °C min^{-1} from room temperature to 200 °C.

Thermogravimetric analysis (TGA) was carried out in a Simultaneous Thermal Analyzer 429 CD/7/G (Netzsch Instruments) equipped with the Data Acquisition System 414/4, under oxygen flow, at a heating rate of 30 °C min^{-1} up to 600 °C.

Dynamic rheological measurements were performed using a RheoStress RS100 (Haake) rotational rheometer with a 20 mm diameter parallel plates geometry at 285 °C under nitrogen atmosphere in oscillatory shear mode, with shear stress 0–400 Pa. A frequency sweep between 0.1 and 100 rad s^{-1} was carried out at a low stress (5 Pa) which was shown to be within the linear elastic range for these materials.

Impact tests were carried out on an Instron Dynatup® 9250HV drop weight tower. All samples were impacted with nominal impact energy of 4.0 J (corresponding to effective impact energy of 5.87 J, as registered by the instrument at the moment of impact). Load versus deflection curves were recorded using an impact striker having a polished hemispherical striking surface with a diameter of 19 ± 0.2 mm, operating with a falling weight of 5.504 kg and a falling speed of 1.21 m s^{-1}, producing an impact energy of 5.87 J.

Scratch tests were carried out on a CSM Micro-Combi Tester using a Rockwell C diamond scratch indenter (tip radius $R = 200$ μm) and by progressively increasing the load from 0.1 to 20 N at a load rate of 6.6 N min^{-1} for a scratch length of 3 mm. This kind of scratch indenter was chosen to produce a sharp scratch on the surfaces. A pre-scan with a very small load was carried out, during which the starting surface profile was measured and subtracted from the loaded scratch scan profile to determine the depth of surface penetration (penetration depth, P_d). The instrument was equipped with an integrated optical microscope and a device to measure the tangential frictional force (in the scratch direction), giving the friction coefficient value during scratching. Three scratches were carried out in different areas for each

specimen and averaged values of the load at which the scratch track appears (critical load, L_c) were determined by optical methods for each analysis.

Shore D hardness was determined by means of a static tester (Affri) according to the ISO 868 standard test method.

Results and discussion

Thermomechanical and rheological characterization

DMTA was used for detecting the mechanical properties and relaxations associated with molecular motions in the filled nanocomposites. The values of T_{alpha} (temperature of the primary mechanical relaxation, as determined from the tanδ peak) and E' are reported in Table 1 for the pristine polymer and for the corresponding composites containing different amounts of nanofillers. Notwithstanding the silica content, the T_{alpha} temperatures detected for the nanocomposites were slightly lower when compared to the pristine PC for the nanocomposites obtained from the A90 and A380 silicas, suggesting that an immobilized or rigid interphase between the bulk polymer matrix and the nanofiller is absent or very limited, as expected due to the hydrophilic nature of the particles' surface and the absence of organic functionalization. The observed small tendency to a decreased T_{alpha} for the PC-nanocomposites compared to the pristine matrix has already been described for PC/carbon nanotubes [15] and for PC/ZnO [16] nanocomposites, as well as for other transparent polymers/Al_2O_3 [11] nanocomposites, and can be attributed to the higher mobility of the PC chains due to the higher free volumes caused by the presence of non-adhering nano-objects inside the polymer bulk. On the contrary, thanks to the organic modification at the surface of the nanofillers, the T_{alpha} values for the nanocomposites obtained from the R972 silica remained almost as high as that of pristine PC. The samples containing 5 vol% of silicas were also tested by DSC to compare the glass transition temperature T_g with the T_{alpha} values obtained by DMTA; the results showed a very good agreement (±2 °C), and this

Table 1 Values of T_{alpha}, elastic and loss moduli as determined by DMTA, and degradation temperature as determined by TGA for PC and PC-silica nanocomposites

Sample	T_{alpha} (°C)	E' at 40 °C (GPa)	$T\text{deg}_{onset}$ (°C)
PC	150.3	0.83	440
PC_A90_1	146.4	1.95	470
PC_A380_1	147.1	1.76	482
PC_R972_1	149.5	2.41	477
PC_A90_2	146.2	2.40	479
PC_A380_2	146.8	2.63	486
PC_R972_2	149.6	2.41	454
PC_A90_5	147.4	1.75	481
PC_A380_5	143.2	2.50	496
PC_R972_5	149.0	2.10	454

confirms the weak interactions existing between the hydrophilic particles and PC, leading to a limited influence on the T_g and T_{alpha} values.

The chemical features of the surface of the nanofillers, along with their primary surface areas, are expected to have some effect on the reinforcement of the PC, because both particle–particle and particle–polymer interactions have been demonstrated to strongly depend on the silica's surface chemistry [17]. In the samples investigated in our work, the DMTA shows a bigger increase in storage modulus for the nanocomposites formed from the organically modified nanosilica R972 at the lower loading (namely 1 vol%), while for the higher loadings (5 vol%) the effect of the particles size overcomes that of the surface chemistry and a more rigid material is obtained from the A380 nanoparticles. This is in agreement with the fact that the organic modification present on R972 nanosilica would lead to a reduction of the so-called Payne effect, based on the particle–particle interaction which is the dominant mechanism of reinforcement for polymer-fumed nanosilica, but which in turn is limited by the organic functionalities at the surface of organically modified silicas [18].

The E' values are, however, not significantly different for the samples containing the unmodified and modified silica nanoparticles. The reason for this is probably that there is already a fairly strong hydrogen bonding interaction between hydroxide groups on the silica and carbonyl groups in the PC. This interaction is strong enough so that changing the wetting characteristics of the silica (as in the case of the R972 silica) does not significantly change the strength of this interaction. It is further interesting to note that, within the series of nanocomposites obtained from one kind of filler by varying amounts, a non-linear relationship is found between the mechanical properties and the silica content. For every kind of silica, the highest values of elastic modulus are observed for 2 vol% of nanofiller loading, while a decrease is observed at the higher loading. This value is very close to the fumed silica concentrations at the percolation threshold reported in the literature for silica-thermoplastics nanocomposites [18–20]. The tendency to aggregation and agglomeration of the nanoparticles at higher loadings was found less significant for the R972 type, as expected due to their hydrophobic and low surface energy character; the higher tendency of R972 to give polymer-particles interaction probably allows the formation of temporary and dynamic PC-silica networks due to the surface modification of the silica particles that facilitate adsorption of the PC molecules on the silica surface. Plots of elastic modulus E' and tanδ are, respectively, shown in Figs. 1 and 2 for the nanocomposites containing 2 vol% of nanofiller, from which it can be concluded that the strong particle–particle interaction is the dominant mechanism in hydrophilic (unmodified) fumed silica nanocomposites, reflected in higher E' values at low temperatures, whereas the organically modified particles–PC interaction is the dominant one when chain motions become allowed at higher temperatures and PC-silica networks are formed.

Table 1 reports the values of the onset temperatures of thermal degradation for the pristine polymer and its nanocomposites containing different amounts of fillers, as obtained from TGA analyses. These results demonstrate a markedly enhanced thermal stability for all the nanocomposites with respect to the corresponding unmodified matrix, confirming the observations by Yang [21] in a comprehensive

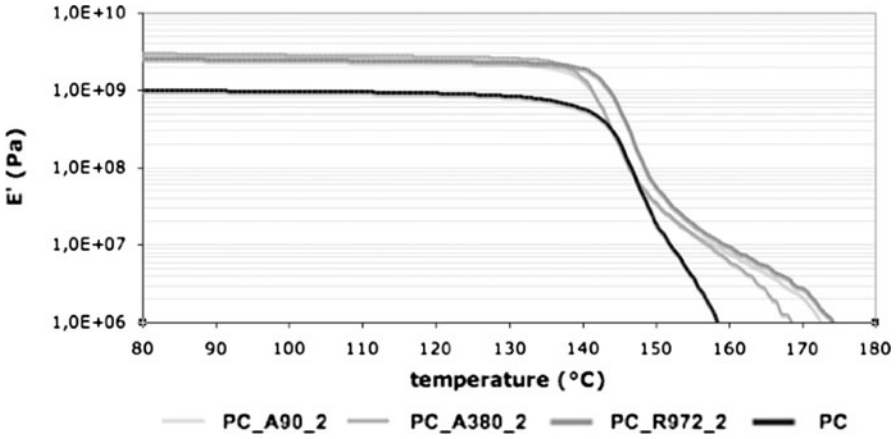

Fig. 1 Elastic modulus (E', GPa) versus temperature of pristine PC and its nanocomposites with 2 vol% of nanofiller

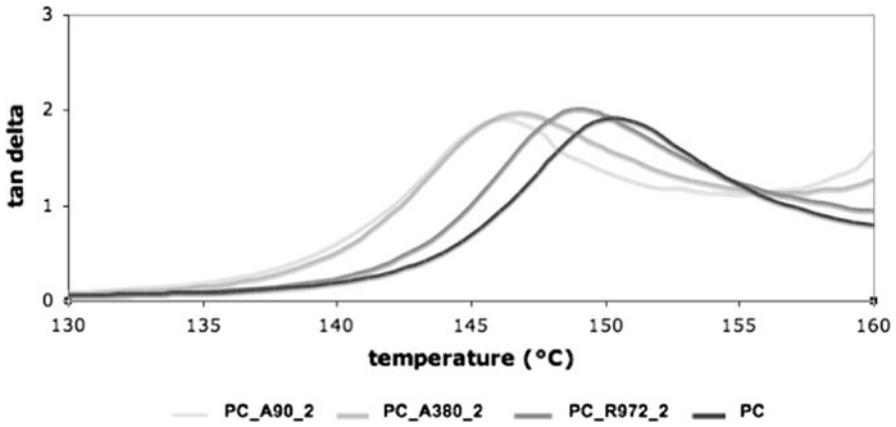

Fig. 2 Tanδ versus temperature of pristine PC and its nanocomposites with 2 vol% of nanofiller

study on the flammability of polymer–silica nanocomposites, where it is clearly stated that, although PC/SiO_2 nanocomposites are not to be considered as flame retardant due to the improvement in thermal stability, less flame retardant additives are needed to achieve the same level of flame retardancy when SiO_2 nanocomposites are used.

The incorporation of nanofillers in molten polymers usually involves a significant change in their viscoelastic properties. Consequently, linear rheology represents a good tool to assess the state of dispersion of fumed silica-polycarbonate nanocomposites directly in the melt state. Due to their fractal structure and their high specific area, coupled with the specific hydroxy functionality on their surface, hydrophilic fumed silica fillers are subjected to a strong particle–particle aggregation and can consequently form a network of interacting particles in the

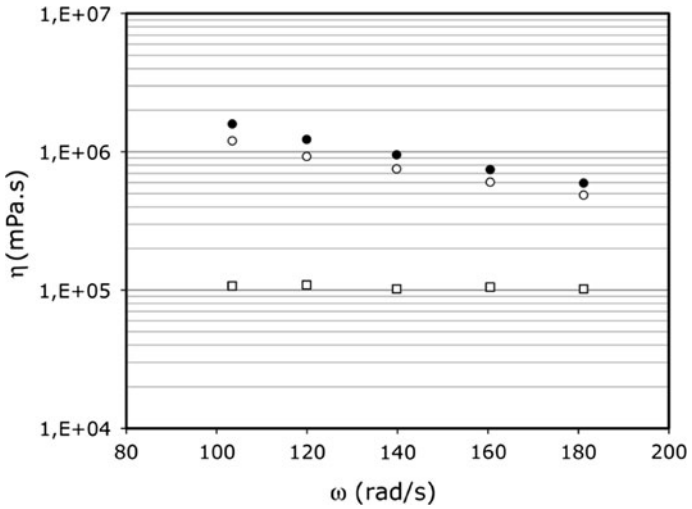

Fig. 3 Complex viscosity (at 285 °C) of pristine PC and its nanocomposites with 5 vol% of nanofiller

molten polymer. A recent review discussed the details of the particles' network development and the nature of particle–polymer interactions with an emphasis on what types of constitutive relations are needed to describe the rheology of fluids containing high aspect ratio nanoparticles [17].

The complex viscosities $|\eta^*|$ of pristine PC and its PC_A90_5 and PC_A380_5 nanocomposites prepared in this study are shown in Fig. 3. The composite materials exhibit a strong shear thinning effect, while the pristine PC shows only a small frequency dependence. The complex viscosity is increased by the presence of the nanoparticles, and their effect is most pronounced at low frequencies; the relative effect diminishes with increasing frequency due to shear thinning. It is interesting to note that the viscosity curves for pristine PC reveal a Newtonian plateau at low frequencies. A fast decrease in the complex viscosities with frequency was observed for both nanofillers. This is in accordance with theoretical expectations and experimental results previously reported for PC nanocomposites [22].

Scratch test

Scratch tests were carried out to investigate the effect of the presence of silica nanoparticles on the scratch resistance of PC. Experiments were done with a load range set from 0 to 2000 mN, and the beginning of the scratch track was taken as representative of the scratch resistance of the material towards penetration. The penetration depth (P_d) values as a function of normal force (F_n) in the range 0–2000 mN are reported in Figs. 4 and 5 for the nanocomposites of the A90 and A380 series.

An impressive improvement of penetration resistance with respect to the pristine PC matrix was observed for all the tested compositions. The slope of the P_d versus F_n curve decreases from about 20 μm N^{-1} for pristine PC to 5–9 μm N^{-1} for PC

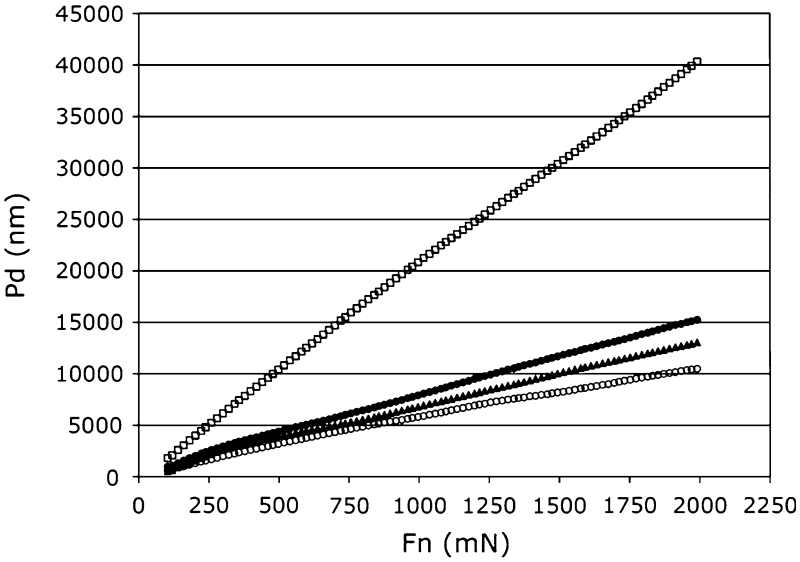

Fig. 4 Penetration depth as a function of normal force in the range 0-2000 mN for PC (*open square*), PC_A90_1 (*filled circle*), PC_A90_2 (*filled triangle*) and PC_A90_5 (*open circle*)

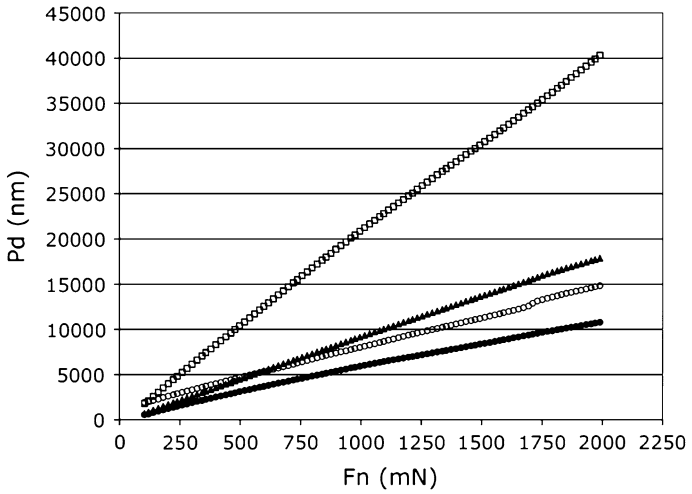

Fig. 5 Penetration depth as a function of normal force in the range 0-2000 mN for PC (*open square*), PC_A380_1 (*filled circle*), PC_A380_2 (*filled triangle*) and PC_A380_5 (*open circle*)

reinforced with both A90 and A380 particles, demonstrating a marked reduction in scratchability due to the reinforcing action of the silicas. The P_d values measured at a normal load of 2000 mN (Pd@2N) are reported in Table 2. A systematic decrease of Pd@2N (from 15.3 to 10.4 μm) was noted by increasing the volume fraction of A90 nanoparticles. A less evident correlation between Pd@2N and silica content was found for nanocomposites containing A380 nanoparticles (in which the lowest

Table 2 Results of scratch test: penetration depth at 2 N (Pd@2N) of load and critical load (L_c)

Code	Pd@2N (μm)	L_c (N)
PC	40.3 ± 10.8	1.8 ± 0.1
PC_A90_1	15.3 ± 2.2	1.2 ± 0.2
PC_A90_2	13.0 ± 0.9	6.2 ± 0.4
PC_A90_5	10.4 ± 0.5	11.8 ± 0.4
PC_A380_1	10.8 ± 0.7	5.6 ± 0.1
PC_A380_2	17.9 ± 2.8	7.2 ± 0.4
PC_A380_5	14.8 ± 3.2	7.9 ± 0.2

penetration was observed for the PC_A380_1 sample). In this case, the very small dimensions of the A380 SiO_2 nanoparticles (average primary particle size of 7 nm) could lead to agglomeration, which in turn would reduce the dispersive mixing of the particles with the polymer because the agglomerates act as if they are solid micro-sized particles.

The scratch resistance was evaluated through the analysis of the critical load, L_c, defined as the normal load at which the scratch track is clearly detectable by optical microscopy. Typical optical micrographs taken after the scratch test are reported in Fig. 6 for unmodified PC and PC_A90_5. The L_c values are reported in Table 2. The scratch resistance of the PC-nanocomposites follows the same trend already discussed for penetration resistance, being strongly enhanced by the addition of silica nanofillers with the exception of PC_A90_1, which shows an unexpected minimum value of $L_c = 1.2$ N. L_c increases from 1.8 N for pristine PC to a maximum of 11.8 N in the case of PC_A90_5. An interesting almost linear correlation between the critical load L_c, representative of scratch resistance, and the volume fraction of the silica nanoparticles was found. In the case of the A90-based nanocomposites, the L_c values increased progressively from 1.2 to 6.2 to 11.8 N for PC_A90_1, PC_A90_2 and PC_A90_5. In the case of the A380-based composites, the L_c values increased progressively from 5.6 to 7.2 to 7.9 N for PC_A380_1, PC_A380_2 and PC_A380_5.

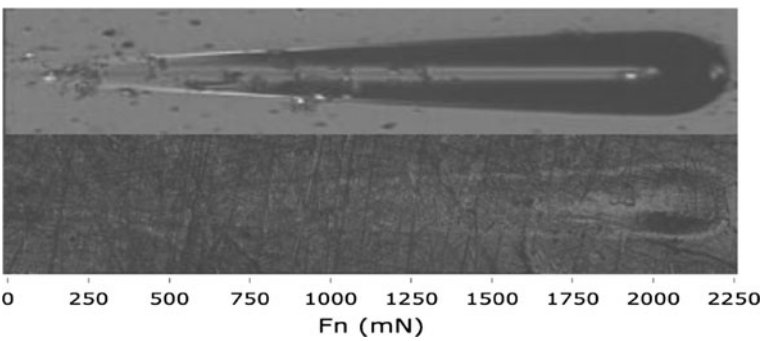

Fig. 6 Optical micrographs after scratch test of PC (*top*) and PC_A90_5 (*bottom*)

Table 3 Shore D hardness of pristine polymers and their nanocomposites

Code	Shore D hardness
PC	56 ± 2
PC_A90_1	65 ± 3
PC_A90_2	72 ± 2
PC_A90_5	73 ± 1
PC_A380_1	76 ± 1
PC_A380_2	72 ± 1
PC_A380_5	75 ± 2

Hardness

The values of Shore D hardness are reported in Table 3 for all the samples. A significant improvement of Shore D hardness with respect to pristine PC was noted in the case of the PC-nanocomposites with both A90 and A380 silicas; the hardness increased from 56 for the pristine matrix up to values ranging between 65 and 76 for composites containing SiO_2 nanoparticles. A straightforward correlation between the hardness and the silica dimension and volume fraction was not observed.

Impact properties

The inherently superior impact properties of PC, combined with the expected toughening effect of the SiO_2 nanoparticles and the high interfacial surface areas available to dissipate energy, suggest that the silica-PC nanocomposites should have excellent potential as high-impact resistant materials. Data obtained by drop-weight impact testing (maximum load, absorbed energy at maximum load and total absorbed energy) are reported in Table 4. The impact performance of the pristine polymer and its nanocomposites was evaluated through the values of maximum absorbed energy (E_{tot}), since this parameter can be considered as a direct index of the mechanical properties modified by the presence of the reinforcing nanoparticles. Data show that the lowest content of nanoparticles shows the greatest improvement of the impact performance of PC, notwithstanding the particle dimensions. As their content increases in the nanocomposites, the maximum absorbed energy decreases.

Table 4 Results of drop-weight impact testing: maximum load (L_{max}), absorbed energy at maximum load ($E_{L_{max}}$) and total absorbed energy (E_{tot})

Code	L_{max} (N)	$E_{L_{max}}$ (J)	E_{tot} (J)
PC	521	1.04	2.59
PC_A90_1	706	1.59	3.45
PC_A90_2	1137	1.64	1.76
PC_A90_5	1329	1.30	2.23
PC_A380_1	1327	4.03	4.11
PC_A380_2	1204	3.36	3.44
PC_A380_5	1307	1.04	1.53

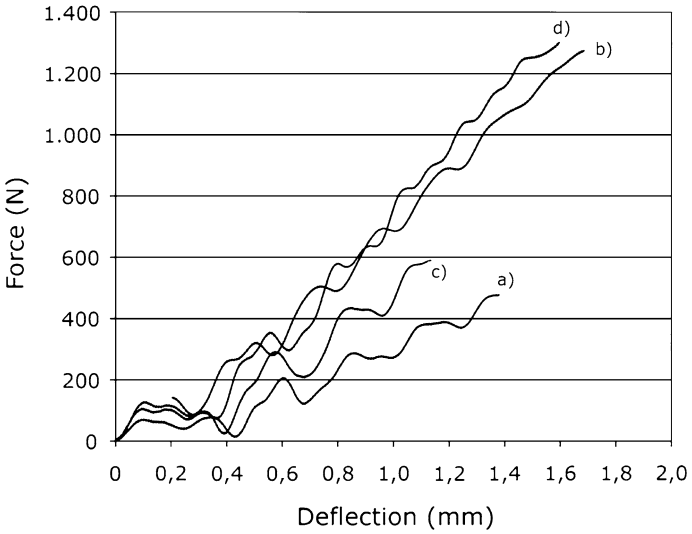

Fig. 7 Impact test: force as a function of deflection for (*a*) PC, (*b*) PC_A380_1, (*c*) PC_A380_2 and (*d*) PC_A380_5

Another important parameter, mainly for ballistic applications, is the maximum load (L_{max}) that can be tolerated by the material during impact events. L_{max} increased from a minimum value of 521 N for pristine PC to values greater than 1300 N for PC_A90_5, PC_A380_1 and PC_A380_5. In the case of the A90 silica a monotonic increment of L_{max} with the volume fraction of reinforcing nanoparticles was noted. In the case of the A380 silica, a linear correlation between maximum load and silica volume fraction was not evident, even though significantly high values of L_{max} were observed for all the samples.

The force–deflection curves derived from impact testing for the A380-nanocomposites compared to the pristine PC are reported in Fig. 7. The dynamic stiffness of the PC-nanocomposites, corresponding to the slope of the curves, strongly increases with respect to the pristine polymer, and a direct correlation with the silica content was found. Similar values obtained for PC_A380_2 and PC_A380_5 suggest the approaching of a threshold beyond which dynamic stiffness is almost blind to particle content. The increase of the dynamic stiffness due to the nanoparticles can be attributed to the presence of an interconnected silica network, which strengthens the material mainly through hydrogen bonding. The ductility of the polymers decreased by increasing the nanoparticle content, and this resulted in lower absorbed energies during impact [23].

Conclusions

Polycarbonate (PC) nanocomposites were prepared by melt mixing in an internal mixer, using a maximum of 5 vol% of either hydrophilic silica nanoparticles with

different primary particle sizes (namely AEROSIL® A380 and AEROSIL® A90), or an organically modified hydrophobic silica (AEROSIL® R972) as reinforcing agents. Notwithstanding the poor interfacial interaction between PC and the hydrophilic silicas, as demonstrated by DMTA analysis, the TGA, scratch test and impact test results show that significant improvements in the PC properties can be obtained even in the absence of organic modification of the silica nanoparticles. In fact, thermal studies revealed an enhanced thermal stability for all the compositions, and rheological investigations showed an increased viscosity for silica nanocomposites with respect to the pristine matrix. A strongly enhanced scratch resistance was found for the PC-nanocomposites ($L_c = 11.8$ N for the best case) with respect to the pristine PC matrix ($L_c = 1.8$ N). Impact properties of PC were also strongly improved by the presence of the silica nanofillers: the maximum load L_{max} increased from 521 N of unmodified PC up to 1329 N for PC containing 5 vol% of A90 silica.

Acknowledgments The authors would like to thank Mrs. Asli Guruscu for help in experimental work. The South African National Research Foundation (GUN62693 and GUN65143), the University of the Free State, and the Italian Ministry of Foreign Affairs (Italy–South Africa bilateral collaboration project N23) are acknowledged for financial support.

References

1. Yoon PJ, Hunter DL, Paul DR (2003) Polycarbonate nanocomposites. Part 1. Effect of organoclay structure on morphology and properties. Polymer 44(18):5323–5339
2. Nayak SK, Mohanty S, Samal SK (2010) Mechanical and thermal properties enhancement of polycarbonate nanocomposites prepared by melt compounding. J Appl Polym Sci 117(4):2101–2112
3. Hong JH, Sung YT, Song KH et al (2007) Morphology and dynamic mechanical properties of poly(acrylonitrile-butadiene-styrene)/polycarbonate/clay nanocomposites prepared by melt mixing. Compos Interfaces 14(5–6):519–532
4. Gonzalez I, Eguiazabal JI, Nazabal J (2006) New clay-reinforced nanocomposites based on a polycarbonate/polycaprolactone blend. Polym Eng Sci 46(7):864–873
5. Lee KM, Han CD (2003) Effect of hydrogen bonding on the rheology of polycarbonate/organoclay nanocomposites. Polymer 44(16):4573–4588
6. Potschke P, Bhattacharyya AR, Janke A et al (2003) Melt mixing of polycarbonate/multi-wall carbon nanotube composites. Compos Interfaces 10(4–5):389–404
7. Potschke P, Bhattacharyya AR (2003) Carbon nanotube filled polycarbonate composites produced by melt mixing and their use in blends. Abstr Pap Am Chem Soc 225:U652–U652
8. Hornbostel B, Potschke P, Kotz J et al (2006) Single-walled carbon nanotubes/polycarbonate composites: basic electrical and mechanical properties. Phys Status Solidi B-Basic Solid State Phys 243(13):3445–3451
9. Chen L, Pang XJ, Yu ZL (2007) Study on polycarbonate/multi-walled carbon nanotubes composite produced by melt processing. Mater Sci Eng A-Struct Mater Prop Microstruct Process 457(1–2):287–291
10. Carrion FJ, Sanes J, Bermudez MD (2007) Effect of ionic liquid on the structure and tribological properties of polycarbonate-zinc oxide nanodispersion. Mater Lett 61(23–24):4531–4535
11. Ash BJ, Siegel RW, Schadler LS (2004) Glass-transition temperature behavior of alumina/PMMA nanocomposites. J Polym Sci B-Polym Phys 42:4371–4383
12. Zhao YQ, Schiraldi DA (2005) Thermal and mechanical properties of polyhedral oligomeric silsesquioxane (POSS)/polycarbonate composites. Polymer 46(25):11640–11647
13. Yang F, Yngard R, Hernberg A et al (2005) Thermal stability and flammability of polymer-silica nanocomposites prepared via extrusion. Fire Polym IV: Mater Concepts Hazard Prev 922:144–154
14. Althues H, Henle J, Kaskel S (2007) Functional inorganic nanofillers for transparent polymers. Chem Soc Rev 36:1454–1465

15. Jin SH, Choi DK, Lee DS (2008) Electrical and rheological properties of polycarbonate/multiwalled carbon nanotube nanocomposites. Colloids Surf A-Physicochem Eng Asp 313:242–245
16. Carrion FJ, Sanes J, Bermudez MD (2007) Influence of ZnO nanoparticle filler on the properties and wear resistance of polycarbonate. Wear 262(11–12):1504–1510
17. Litchfield DW, Baird DG (2006) The rheology of high aspect ratio nano-particle filled liquids. Rheol Rev (2006):1–60
18. Paquien JN, Galy J, Gérard JF, Pouchelon A (2005) Rheological studies of fumed silica-polydimethylsiloxane suspensions. Colloids Surf A-Physicochem Eng Asp 260(1–3):165–172
19. Cassagnau P (2003) Payne effect and shear elasticity of silica-filled polymers in concentrated solutions and in molten state. Polymer 44(8):2455–2462
20. Inoubi R, Dagreou S, Lapp A et al (2006) Nanostructure and mechanical properties of polybutylacrylate filled with grafted silica particles. Langmuir 22(15):6683–6689
21. Yang F, Yngard R, Nelson GL (2005) Flammability of polymer-clay and polymer-silica nanocomposites. J Fire Sci 23(3):209–226
22. Kitano T, Kataoka T (1980) The effect of the mixing methods on viscous properties of polyethylene melts filled with fibers. Rheol Acta 19(6):753–763
23. Gustin J, Freeman B, Stone J et al (2005) Low-velocity impact of nanocomposite and polymer plates. J Appl Polym Sci 96(6):2309–2315